DOI: 10.1002/anie.201001623

Particles at Interfaces

Synthesis of Nano/Microstructures at Fluid Interfaces

Zhongwei Niu, Jinbo He, Thomas P. Russell, and Qian Wang**

Keywords:
colloidosomes · hierarchical structures · interfacial assembly · interfacial reactions · Janus structures

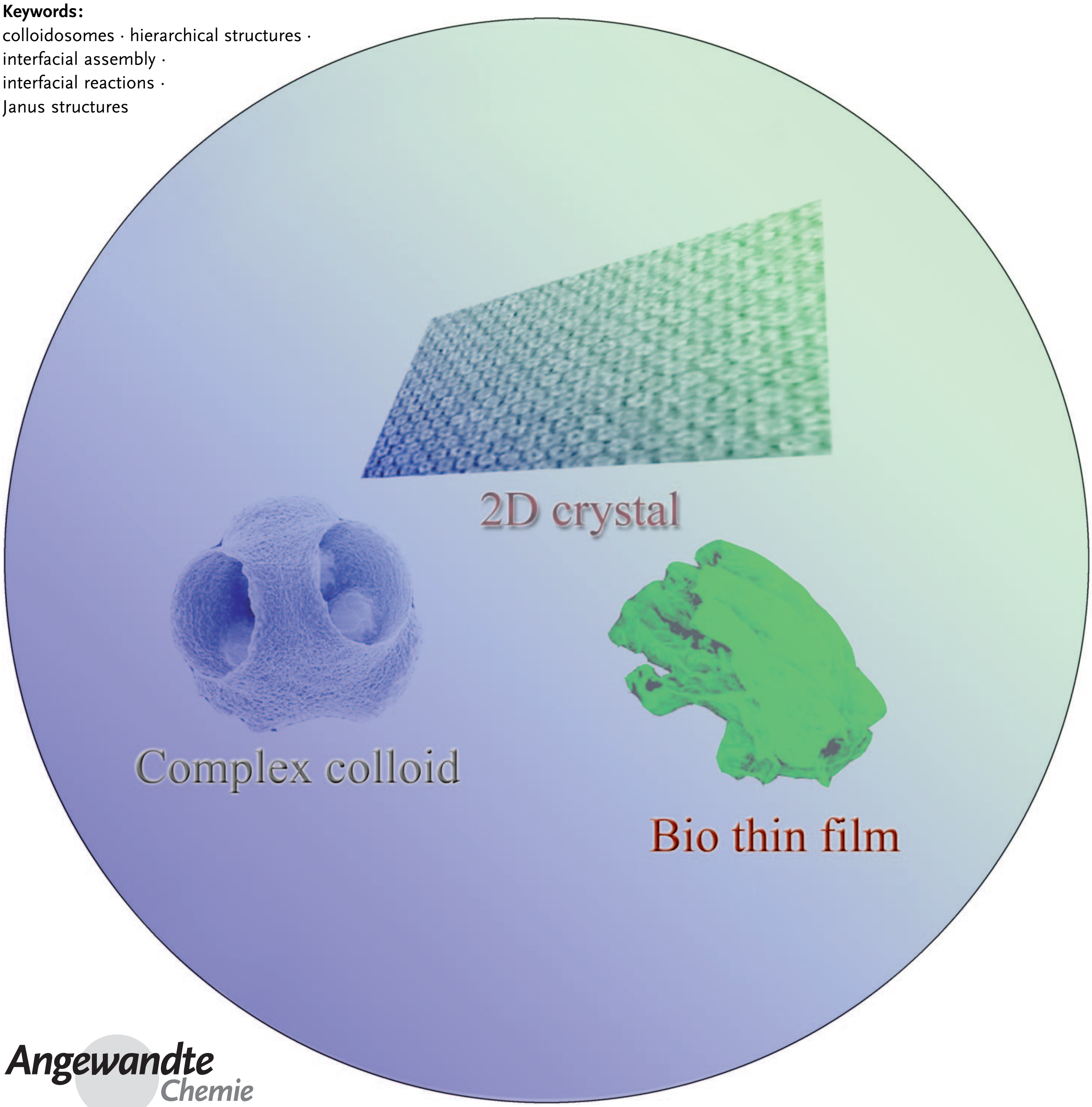

The generation of novel multifunctional materials with hierarchical ordering is a major focus of current materials science and engineering. For such endeavors, fluid interfaces, such as air–liquid and liquid–liquid interfaces, offer ideal platforms where nanoparticles or colloidal particles can accumulate and self-assemble. Different assembly processes and reactions have been performed at fluid interfaces to generate hierarchical structures, including two-dimensional crystalline films, colloidosomes, raspberry-like core–shell structures, and Janus particles, which lead to broad applications in drug delivery and controlled release, nanoelectronics, sensors, food supplements, and cosmetics.

From the Contents

1. Introduction

The focus of nanoscience and nanotechnology is gradually shifting from the synthesis of individual components to their assembly into large-scale systems of nanostructured materials. In general, organized nano-/microstructures show remarkable collective properties with great potential in applications such as nanoelectronics, sensing, and diagnostics. Many of these applications are not based on individual particles but rather on their assemblies in which they interact with each other and organize hierarchically. Two general approaches can be employed to form multidimensional organized nano/microstructures: top-down approaches, such as lithography[1] and microcontact printing,[2] and bottom-up approaches, such as self-assembly.[3] Among different self-assembly strategies, the assembly of particles at air–liquid and liquid–liquid interfaces offers a promising method to organize nanoparticles or colloidal particles in a well-defined manner.[4,5]

The self-assembly of particles at curved fluid interfaces was first reported by Pickering[6] and Ramsden[7] about a century ago. Emulsions stabilized by colloidal particles are thus known as Pickering emulsions. As the energetic penalty associated with the formation of an interface is given by the product of the total area of the interface and the interfacial energy, particles dispersed in one of the phases will segregate to an interface so as to mediate interactions between the fluids. Consequently, the segregation of particles to the interface acts to stabilize the interface. Until now, this technique has been used to produce supracolloidal structures, such as permeable hollow capsules, colloidosomes, colloid-based, nanoparticle-armed polymer latex, complex gels, and Janus structures.[4,5] Flat interfaces have also been employed as a constrained environment to generate two-dimensional (2D) self-assemblies of nanoobjects with long-range orders.[8,9] Furthermore, the basic concept can be used to assemble viral particles and other biological nanoparticles and form biological capsules and thin films upon cross-linking at interfaces.[4,10]

Interparticle interactions, including capillary, dipolar electrostatic, and elastic forces, govern the self-assembly of solid particles at interfaces. As these interactions and the basic theory describing the assembly are well-documented and reviewed,[3–5,11–18] in this Review we will focus on the structures generated by the self-assembly of nanoparticles or colloidal particles at interfaces.

2. Thermodynamic Model of Particles at Interfaces

Why do the particles segregate to liquid interfaces? Pieranski first provided a description of spherical colloidal particles assembled at interfaces in terms of the decrease in the total free energy of the system approximately 70 years after Pickering's discovery.[19] As shown in Figure 1, the placement of a single particle with an effective radius r at the interface between oil (O) and water (W) leads to a decrease of the energy of the system from E_0, the energy arising from the interface between the liquids, to E_1, the energy with particles located at the interface, yielding an energy difference ΔE [Eq. (1)]:

---

[*] Prof. Q. Wang
Department of Chemistry and Biochemistry
University of South Carolina
631 Sumter Street, Columbia, SC 29208 (USA)
E-mail: wang@mail.chem.sc.edu
Homepage: http://www.chem.sc.edu/faculty/wang/
Prof. Z. Niu
Technical Institute of Physics and Chemistry
Chinese Academy of Sciences
No.2 Beiyitiao Street, Zhongguancun, Beijing 100190 (China)
Dr. J. He, Prof. T. P. Russell
Department of Polymer Science and Engineering
University of Massachusetts Amherst
120 Governors Drive, Amherst, MA 01003 (USA)
E-mail: russell@mail.pse.umass.edu

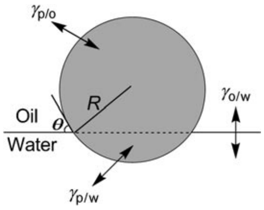

Figure 1. An isotropic particle at the oil–water interface.

$$E_0 - E_1 = \Delta E = -\frac{\pi r^2}{\gamma_{O/W}}\left[\gamma_{O/W} - (\gamma_{P/W} - \gamma_{P/O})\right]^2 \qquad (1)$$

Here, two main factors dominate, namely the size of particle r and the wettability of particle surface, which is determined by the particle–oil interfacial energy $\gamma_{P/O}$, the particle–water interfacial energy $\gamma_{P/W}$, and the oil–water interfacial energy $\gamma_{O/W}$.

Generally, for microscopic particles (colloidal particles), the decrease in total free energy is much larger than thermal energy ($k_B T$), which leads to an almost permanent effective confinement of large colloids to the interface. However, nanoscopic particles are confined to the interface by an energy reduction comparable to thermal energy. Consequently, the assembly of nanoparticles at liquid interfaces is dynamic, with particles adsorbing to and desorbing from the interface. The desorption of particles from the interface is expected to be exponential with time, with a characteristic time τ_{off} that should increase with the adsorption free energy ΔE as $\tau_{off} = A\exp(-\Delta E/k_B T)$, with A being only weakly dependent on size.[20] Therefore, nanoparticles are easily displaced from the interface, with a constant particle exchange with the mother liquor, the rate of which depends on particle size. The interfacial behaviors of various colloidal systems with particles of different size and surface chemistries (for example, polystyrene (PS) lattices, silica particles) have been described in the literature.[21–25] Moreover, similar studies of nanoparticles at interfaces have also been performed in detail for the purpose of constructing hierarchically organized structures.[26–29]

The wettability of a particle surface is described by the contact angle θ between the particle surface and the oil–water interface (Figure 1). This contact angle greatly affects the stabilities of the oil-in-water or water-in-oil emulsions. In general, to make stable emulsions, the less-wetting liquid should be the dispersed phase.[30] For example, Binks and Lumsdon demonstrated that using a toluene/water system, which has an interfacial tension of 36 mN m^{-1}, 10 nm-diameter silica nanoparticles, having different wettabilities based on surface functionality, showed a maximum in desorption energy and has at a contact angle of 90°.[21] Increasing or decreasing the contact angle decreases the stability of the emulsion.[31] The stabilizing effect described above applies only for particles with homogeneous wettability.

Zhongwei Niu completed his PhD in chemistry in 2003 from Institute of Chemistry, Chinese Academy of Sciences (CAS), under the supervision of Prof. Zhenzhong Yang. In 2004, he joined the group of Prof. Eric Nies at the University of Leuven as a postdoctoral fellow. In 2005, he moved to Prof. Qian Wang's group at the University of South Carolina. In 2008, he worked as the research assistant professor at the University of South Carolina. Since 2009, he has been a professor at the Technical Institute of Physics and Chemistry, Chinese Academy of Sciences. His research interests include the self-assembly of bionanoparticles and biomaterials development.

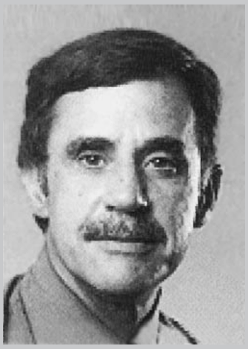

Thomas P. Russell received his PhD in 1979 in polymer science and engineering from the University of Massachusetts Amherst. Between 1981 and 1996 he was a researcher at the IBM Almadewn Research Center in San Jose, CA, and was made Silvio O. Conte Distinguished Professor of Polymer Science and Engineering at the University of Massachusetts Amherst in 1997. He is the Director of the Energy Frontier Research Center on Polymer-Based Materials for Harvesting Solar Energy, an Associate Director of MassNanoTech, and an Associate Editor of Macromolecules. He is a fellow of the American Physical Society, the American Association for the Advancement of Science, and the Neutron Scattering Society of America, and is a member of National Academy of Engineering.

Jinbo He completed his Bachelor's and Master's degrees in polymer chemistry and physics at Nanjing University in China. In 2008, He received his PhD degree from Department of Polymer Science & Engineering at the University of Massachusetts in Amherst under the supervision of Prof. Thomas P. Russell. He is currently a postdoctoral scholar in Prof. Heinrich M. Jaeger's group at the University of Chicago. His current research interests include self-assembly of nanoparticles at interfaces, related nanomechanic, electric, magnetic, and diffusive properties of nanoparticle membranes, and giant electrorheological effects of nanoparticles.

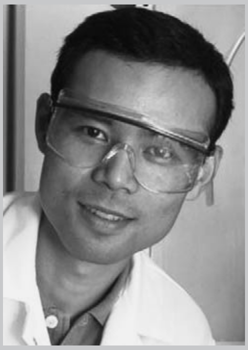

Professor Qian Wang received his PhD in organic chemistry from Tsinghua University in 1997 under Prof. Yufen Zhao. After postdoctoral experiences with Prof. Manfred Schlosser at the University of Lausanne (1997–1999) and Prof. M. G. Finn at the Scripps Research Institute (1999–2003), he started as an Assistant Professor at the University of South Carolina in 2003, where he is currently the Robert L. Sumwalt Professor of Chemistry. His research interests focus on creating 3D programmable scaffolds to probe cellular activities. He is also interested in bioconjugation chemistry and the development of protein markers and enzyme inhibitors by combinatorial synthesis.

Apart from a surface with homogeneous wettability, particles with inhomogeneous surface properties (Janus particles, for example) could be reported thanks to recent synthetic advances.[32–43] A Janus particle is defined as having two distinctly different surface regions; polar and apolar regions are the most common examples, as shown in Figure 2. Such a particle is characterized by two contact angles: θ_P, the contact angle of the polar region, and θ_A, the contact angle of the apolar region.

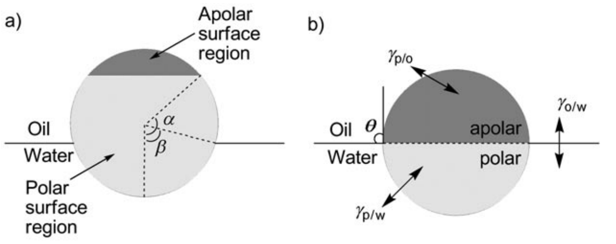

Figure 2. a) A Janus particle at the oil–water interface. The relative areas of the polar and apolar particle surface regions are parameterized by the angle α. β denotes the immersion angle of the particle at the oil–water interface. Reprinted from Ref. [32] with permission. Copyright 2001 American Chemical Society. b) A Janus particle with equal polar and apolar regions lying at the oil–water interface.

The contact angles θ_A and θ_P correspond to the equilibrium contact angles given by Young's equation [Eqs. (2) and (3)]:

$$\cos\theta_A = \frac{\gamma_{A/W} - \gamma_{A/O}}{\gamma_{O/W}} \tag{2}$$

$$\cos\theta_P = \frac{\gamma_{P/W} - \gamma_{P/O}}{\gamma_{O/W}} \tag{3}$$

Here, $\gamma_{A/W}$, $\gamma_{A/O}$, $\gamma_{P/W}$, $\gamma_{P/O}$, and $\gamma_{O/W}$ refer to the interfacial energies of the apolar–water, apolar–oil, polar–water, polar–oil, and oil–water interfaces, respectively. The amphiphilicity of a Janus particle can be tuned by 1) variation of the angle α (different composition fractions) or 2) changing the surface properties of the two areas (difference between the two contact angles θ_A and θ_P). The maximum amphiphilicity is expected in the case of $\alpha = 90°$ and $\theta_A - \theta_P = 180°$. This case corresponds to a Janus particle consisting of equal polar and apolar surface regions in which the polar region is completely wetted by water and the apolar region is completely wetted by oil (Figure 2b). In this case, the desorption energy is several times larger than that for a comparably sized homogeneous particle, as discussed by Binks and Fletcher.[32]

For nanoparticles with anisotropic shapes, for example nanorods, the same thermodynamic arguments apply (neglecting variation in the contact angle around the perimeter of the particle). Other factors, such as concentration, pH value, and ionic strength (for charged nanoparticles), can influence the orientation of nanorods at the interface along with the separation distance and long-range ordering. The concentration of nanorods in solution limits the total number of nanorods that can assemble at the interface, which is determined by the chemical potential difference of the nanorods at the interface and in the bulk solution, similar to spherical nanoparticles.[45] At low concentrations of nanorods, individual nanorods segregate at the interface and orient parallel to the plane of the interface so as to maximize the reduction in energy (Figure 3a).[44,46] As the concentration of nanorods in the bulk solution increases, the interfacial tension decreases until the interface is saturated with randomly packed nanorods oriented parallel to the interface. Additionally, nematic or smectic phases (determined by the aspect ratio of nanorods) can be induced at this stage due to the dynamic particle exchange between the interface and bulk solution. Upon further increasing the concentration of nanorods, the separation distance between the nanorods decreases to a critical point at which nanorods are forced to reorient normal to the interface so as to further reduce the energy of the system.[44,46] As the particle size gets smaller, contribution from the line tension has to be considered, as demonstrated by Johnson and Dong.[47]

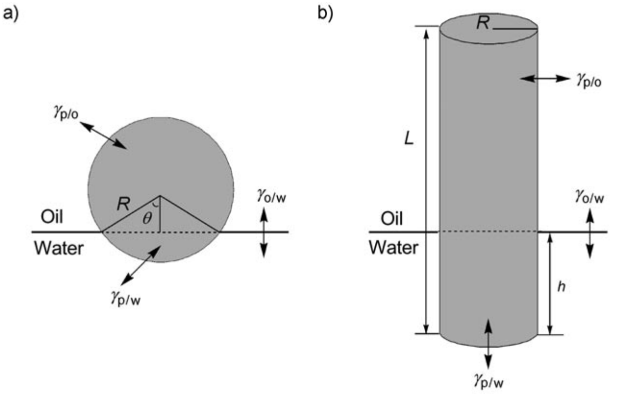

$$\Delta E_{\parallel} = -2RL\sin\theta\gamma_{o/w} + 2RL\theta(\gamma_{p/w} - \gamma_{p/o}) \qquad \Delta E_{\perp} = (\gamma_{p/w} - \gamma_{o/w} - \gamma_{p/o})\pi R^2 + (\gamma_{p/w} - \gamma_{p/o})2\pi Rh$$

$$\text{Where} \quad \cos\theta = \frac{\gamma_{p/w} - \gamma_{p/o}}{\gamma_{o/w}} \quad (L >> R)$$

Figure 3. Nanorods oriented parallel (a) and perpendicular (b) to the oil–water interface. $\Delta E_{\parallel}$ is the energy change when the nanorods are parallel to the interface, and $\Delta E_{\perp}$ is the energy change when the nanorods are perpendicular to the interface. *R* and *L* are the effective radius and length of the rods, respectively, and γ is the interfacial energy. *P*, *O*, *W*, and θ represent the particle, oil (toluene), water, and the contact angle of the particle at the interface, respectively. *h* is the penetration depth of the nanorods into the water phase when placed normal to the interface. Reprinted from Ref. [44].

Besides the traditional surface-tension arguments, another scenario has been reported for highly charged particles. Chaikin and co-workers reported that when poly(methyl methacrylate) particles were suspended in bromocyclohexane, which is an oil with a relatively high dielectric constant, these hydrophobic nonwetting particles can be strongly bound to oil–water interfaces because of image charge effects (Figure 4).[48] The particles sit on the interface but not at the interface, so the surface tension argument does not apply in this case. The net interaction between the water

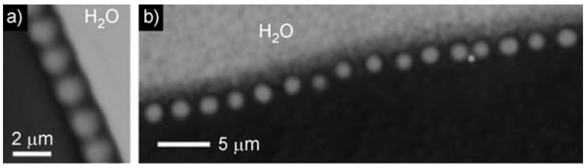

Figure 4. PMMA particles (radius 1.08 μm) in bromocyclohexane/decalin permanently bound at the oil–water interface and in various configurations. a, b) Close-up images taken perpendicular to the interface. The water phase was imaged in bright-field transmission mode (a) or by dissolving fluorescent dye into the solution (b). Reprinted from Ref. [48] with permission.

droplet and the colloidal particle V can be represented by Equation (4):

$$V(d)=\frac{Z}{\varepsilon_m\varepsilon_0}\left(\frac{Q}{d}-\frac{ZR}{R^2-d^2}\right) \tag{4}$$

Here ε_m is the dielectric constant of oil, Z is the charge on the colloidal particle, Q is the charge of the water droplet, R is the radius of the water droplet, and d is the distance of colloidal particles from the center of the water droplet. Similar to the manner in which a charged particle approaches the surface of a conductor, an image charge of opposite sign appears at the mirror position and resulting in an attraction of the particle to the interface. When charged colloidal particles are dispersed in a low dielectric constant medium (oil) and they approach a conducting medium (such as water), an image charge attraction dominates and traps the particles on the interface.

3. Thin Films at Fluid Interfaces

3.1. Thin Films at Air–Liquid Interfaces

Interfaces provide a constrained environment for organized assemblies of nanoparticles. For example, both the air–liquid and liquid–liquid interfaces have been widely exploited for the preparation of thin films of metals or semiconductors.[4,8,9,49] In particular, at the air–liquid interface (as in a Langmuir trough), thin films of CdSe quantum dots,[50] platinum nanoparticles,[51] gold clusters,[52] silver nanoparticles,[53] magnetic Fe_3O_4 nanoparticles,[54] $BaCrO_4$ nanorods,[55] ZnS nanorods,[56] silver nanowires,[57] and carbon nanotubes[58] have been prepared. Furthermore, Langmuir–Blodgett (LB) techniques, that is, the transfer of an assembly at the water–air interface to a solid surface, has been broadly used to achieve closely packed thin films.[9] In the LB technique, a Langmuir monolayer is initially prepared on the air–liquid interface. By compressing the monolayer, the packing of the Langmuir film can be tuned (Figure 5). The orientation of components comprising the monolayer is influenced by the surface pressure. The monolayer can then be deposited onto a solid substrate by vertical-dipping or horizontal-lifting techniques. Lee and Tsai recently discussed the preparation of monolayers of close-packed gold nanoparticles by combining the self-assembly of gold nanoparticles at interface and LB techniques.[59] In their approach, a positively charged octadecylamine monolayer at the air–water interface was used as a template layer to adsorb negatively charged gold nanoparticles to the interface from the aqueous phase. Ordered domains of gold nanoparticles were then formed at the air–liquid interface. A close-packed monolayer of the nanoparticles was obtained by compression and could be transferred onto a solid surface by vertical dipping.[59]

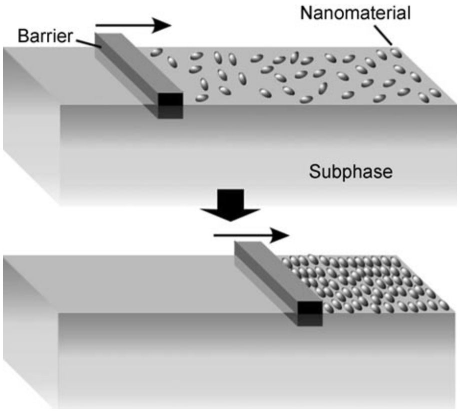

Figure 5. Compression of nanomaterials by barrier motion at the air–water interface. Reprinted from Ref. [9].

In addition to spherical nanoparticles, one-dimensional (1D) nano-objects, such as nanorods, nanowires, and nanotubes, can also self-assemble at the air–liquid interface. Technically speaking, assembling these 1D nanoscale building blocks into various architectures with defined orientation and interparticle spacing is more challenging, but can lead to many applications, including high-performance optoelectronic devices, field-effect transistors, logic circuits, and biosensors.[60–62] Yang and co-workers reported the fabrication of short-aspect-ratio $BaCrO_4$ nanorods thin films at the air–liquid interfaces.[55] At various surface pressures, the structures of these assemblies varied from raft-like aggregates to partially nematic or smectic arrangements to multilayers of nematics (Figure 6). Acharya and Efrima reported that ZnS nanorods could organize in side-by-side and end-to-end manner by self-assembly at an air–liquid interface by applying 2D surface pressures.[56] A similar strategy was used to assemble silver nanowires,[57] silicon nanowires,[63] and single-walled carbon nanotubes.[58,64]

3.2. Thin Films at Liquid–Liquid Interfaces

In comparison to the liquid–air interface, liquid–liquid interfaces have not been investigated extensively. Nanoparticles are highly mobile at the liquid–liquid interface and can rapidly achieve an equilibrium assembly. Furthermore, the high fluidity of the interface enables a self-correction of defects and a rich, 2D phase-separation behavior. In general, three parameters influence nanoparticles assembling at the liquid–liquid interface: the nature of the interface, the surface properties of the nanoparticles, and the effective radius of the nanoparticles.[8]

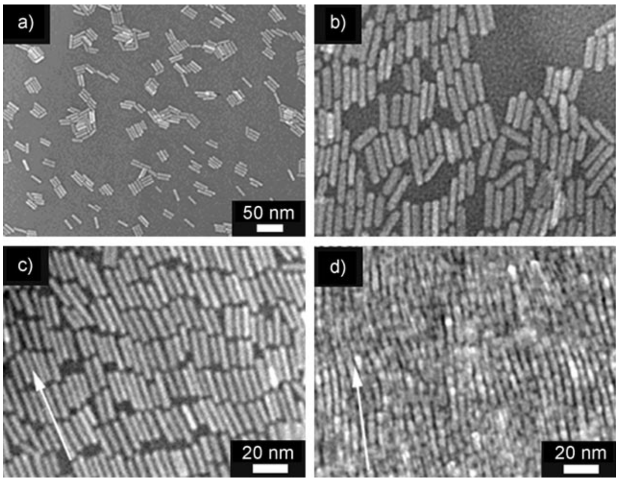

Figure 6. TEM images of $BaCrO_4$ nanorods assembled at the water–air interface at different stages of compression: a) isotropic distribution at low pressure; b) monolayer with partial nematic arrangement; c) monolayer with smectic arrangement; and d) nanorod multilayer with nematic configuration. Modified image; reprinted from Ref. [55] with permission. Copyright 2001 American Chemical Society.

Recently, great progress has been made in the preparation of thin films of nanoparticles at liquid–liquid interfaces. For example, Wang and Xia successfully fabricated freestanding, close-packed gold nanoparticle thin films by use of the water–oil interface.[65] Here, citrate-stabilized negatively charged 12 nm gold nanoparticles were found to self-assemble into a monolayer at the pentanol–water interface. A small amount of ethanol or a gentle shaking can accelerate the assembly process. Free-standing gold nanoparticle thin films were obtained after removing the pentanol and heating to 48°C for 3 h (Figure 7a–d). Jaeger and co-workers demonstrated that highly ordered two-dimensional gold nanoparticle films could be fabricated by a simple direct-drying method, either at the toluene–water interface or toluene–air interface (Figure 7e,f).[66,67] Other ligand-capped gold nanoparticles,[26,68] FePt nanoparticles,[69] silver nanoparticles,[70] $CoPt_3$ nanoparticles,[71] and γ-Fe_2O_3 nanoparticles[26] can also self-assemble at the oil–water interface and form thin films.

Rotello and co-workers reported an alternative method to prepare stable magnetic thin films at the oil–water interface.[69] To stabilize the terpyridinethiol-functionalized FePt nanoparticles at the water–toluene interface, coordination chemistry was used to cross-link the nanoparticles in situ at the interface. Terpyridine can form stable complex with iron(II) ions. Furthermore, highly ordered monolayer graphene nanosheet films,[72] thin films of single-walled carbon nanotubes,[73–77] and oriented films of layered rare-earth hydroxide crystallites[78] have also been successfully fabricated at water–oil interfaces.

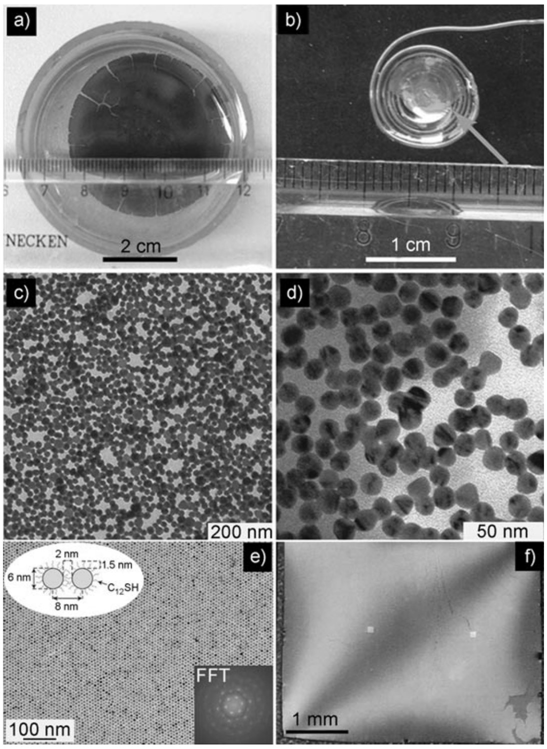

Figure 7. a) Optical image of a free-standing monolayer film of 12 nm gold NPs. The film was obtained by self-assembly of the NPs at the water–pentanol interface in a Petri dish, followed by heating at 48°C for 3 h. b) Optical image of the dried film obtained by transferring the film shown in (a) onto a copper loop. The film is indicated by an arrow. c) Low- and d) high-magnification TEM images of the resulting films. Reprinted from Ref. [65]. e) TEM of a typical monolayer produced by drop-casting 10 μL of a solution of dodecanethiol-ligated 6 nm gold nanocrystals onto a 3×4 mm^2 SI_3N_4 substrate. f) Top view of a fully formed, compact nanocrystal monolayer on the top surface of a thin liquid droplet. Modified image; reprinted from Ref. [67] with permission. Copyright 2007 Macmillan Publishers Ltd: Nature Materials.

4. Colloidosome Structures

Colloidosomes are microcapsules that have a shell composed of densely packed colloidal particles or nanoparticles. These structures are typically generated from Pickering emulsions. After cross-linking the particles at the interface, stable colloidosome structures can thus be readily prepared. This strategy has been used to prepare a large range of colloidosomes with particles ranging in size from several nanometers to several micrometers in diameter. The physical properties of these colloidosomes, such as the mechanical strength and permeability, can be tuned by the choice of the particles, interfacial properties of the particles, and other preparation conditions. The hierarchical assemblies produced allow for encapsulation or controlled-release applications.

Velev and co-workers first reported the production of such supracolloidal structure in 1996.[79] In 2002, Dinsmore et al. named this supracolloids as colloidosomes.[80] They demonstrated a three-step procedure to prepare colloidosomes: An aqueous solution was first added to an oil containing the colloidal particles. Then, by continuously shearing for several seconds, stable emulsions were formed with the particles adsorbed onto the surface of the droplet. These assemblies were then fixed by the addition of polycations, by use of van der Waals forces, or by sintering the particles (Figure 8). The colloidosome, of course, has

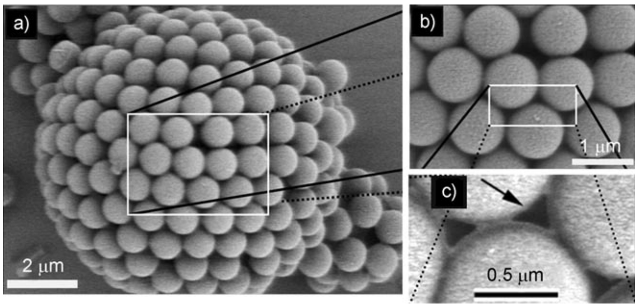

Figure 8. a) Scanning electron microscope image of PS colloidosomes. b,c) Close-up views. The arrow points to one of the 0.15 µm holes that define the permeability. Reprinted from Ref. [80] with permission. Copyright 2002 American Association for the Advancement of Science.

interstitial pores between the spheres packed at the interface, which were shown to be permeable to small objects but not to particles having a diameter larger that the size of these interstitial pores. These colloidosome capsules are very tough, which was confirmed by measurements of the internal osmotic pressure and shell stiffness.[81] A similar approach was used by Croll et al. to prepare colloidosomes with 0.6 µm poly(divinylbenzene-*alt*-maleic anhydride) particles.[82] He et al. also described the production of colloidosomes with sulfonated PS particles.[83–85] Furthermore, poly(methyl methacrylate-*co*-acrylic acid) latex particles could be used to generate pH-sensitive colloidosomes.[86]

In addition to colloidal particles, nanoparticles, and nanorods, such as silica nanoparticles,[87–90] CdSe nanoparticles,[27,91] CdSe/ZnS nanoparticles,[92] gold nanoparticles,[93,94] Fe_3O_4 nanoparticles,[95,96] single-walled carbon nanotubes,[97,98] and CdSe nanorods,[44] can also self-assemble at immiscible fluid interfaces to produce stable emulsions. To obtain mechanically stable capsules from the nanoparticle assemblies, the absorbed nanoparticles need to be fixed at the interface. This fixing can be achieved by the use of ligands attached to the nanoparticles; the ligands can be cross-linked either by photolytic or chemical reactions. Skaff et al. used a ring-opening metathesis polymerization on CdSe/ZnS core–shell nanoparticles having ligands with a norbornene derivative, making use of a water-soluble PEGylated Grubbs catalyst.[92] After cross-linking, stable well-defined CdSe/ZnS capsules were obtained. Very recently, a copper(I)-catalyzed Huisgen reaction was reported to cross-link alkyne- and azide-functionalized Fe_3O_4 nanoparticles at the water–oil interface.[95] Two major advantages of this strategy are: 1) the reaction between alkyne and azide functional groups is highly selective and essentially inert to the many functional groups and environmental conditions, and 2) it provides a dense packing of nanoparticles on the colloidosome shell, resulting in high-stability colloidosomes.[95]

It has been reported the residence time of the nanoparticles at the interface decreases with decreasing size of the nanoparticles,[27] which varies with the square of the particle radius. This size-dependent energy can be used to displace smaller nanoparticles assembled at the interface by larger ones. Russell and co-workers showed that 4.6 nm CdSe can displace 2.8 nm CdSe at the oil–water interface and, in fact, a 2D phase separation occurs at the interface based on the size of the nanoparticles (Figure 9).[27] Recently, co-assembly of multicomponent colloidal particles with different surface properties has also been reported.[99]

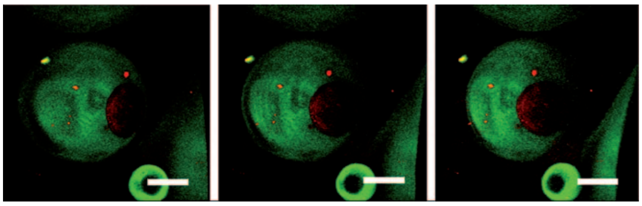

Figure 9. Three-dimensional reconstructions of confocal microscopic images showing a dispersion of water droplets stabilized by 2.8 nm diameter CdSe nanoparticles (green) after the introduction of a solution of 4.6 nm diameter CdSe nanoparticles (red). The three images are the same volume of the sample rotated in the field of view. The 4.6 nm nanoparticles displace the 2.8 nm nanoparticles and show evidence of a phase separation on the water droplet surface. Scale bar: 16 µm. Reprinted from Ref. [27] with permission. Copyright 2003 American Association for the Advancement of Science.

Kumacheva and co-workers have reported the preparation of monodisperse colloidosomes by an inside-out microfluidic approach.[100,101] Weitz and Lee recently reported a facile approach to prepare complex colloidosome structures by using a glass capillary microfluidic device.[102,103] In their approach, double emulsions with a core–shell geometry were first generated using a glass capillary microfluidic device. Hydrophobic silica nanoparticles dispersed in the oil shell can stabilize the droplets and ultimately become the colloidosome shells upon removal of the oil solvent. The size of the colloidosomes could be precisely tuned by independently controlling the flow rates of each fluid phase.[102] Another great advantage of this method is that the colloidosomes are generated in a continuous phase of water, which can avoid the transfer of the colloidosomes from an oil to an aqueous phase. Moreover, nonspherical colloidosomes with multiple compartments were also fabricated by double emulsions templates (Figure 10).[103] In this approach, a glass capillary microfluidic device that combines a co-flow and a flow-focusing geometry is used to generate double emulsions with controlled morphologies. Hydrophobic SiO_2 nanoparticles suspended in the oil phase and poly(vinyl alcohol) dissolved in the aqueous phase stabilized the double emulsions. During the oil removal, the internal water–oil interface retained its spherical shape, whereas the outer water–oil interface deformed.

5. Raspberry Structures from Colloids or Nanoparticles

A raspberry structure consists of nanoparticles or colloidal particles that decorate the surface of a solid core. Most efforts to prepare such structures use the oil–water interface as the template and can be divided into two approaches: 1) Pickering emulsion polymerization, and 2) aqueous-phase gelation.

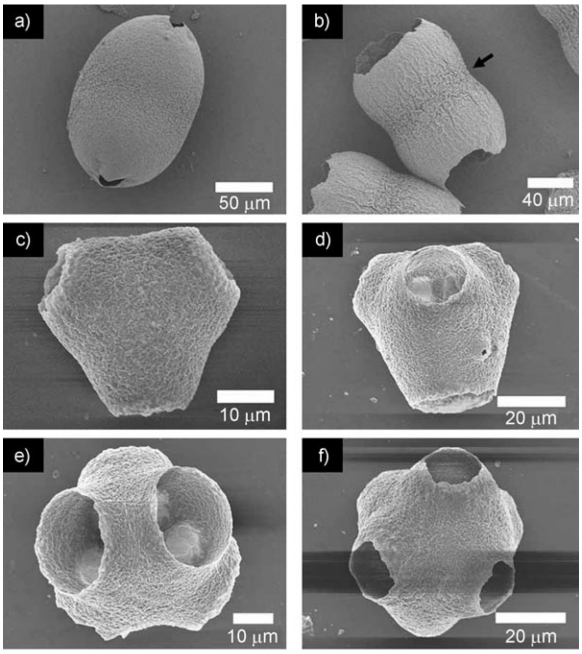

Figure 10. SEM images of nonspherical colloidosomes generated with varying number of internal drops. a,b) $n=2$ with a) ellipsoid and b) peanut structures, c) $n=3$, d) $n=4$, e) $n=5$, and f) $n=6$, where n is the number of the internal aqueous drops in the emulsion drop. Reprinted from Ref. [103].

5.1. Pickering Emulsion Polymerization

Emulsion polymerization techniques have been widely used to fabricate fascinating colloidal structures, such as core–shell or hollow latex structures. If the conventional surfactant is replaced with nanoparticles or colloidal particles, a stable Pickering emulsion can also be formed. If the nanoparticle- or colloidal-particle-stabilized inner phase is substituted with a monomer solution with an initiator or oxidant, the monomer can be polymerized, leading to a sphere of polymer decorated with either nanoparticles or colloidal particles. This surfactant-free solid-particle-stabilized emulsion polymerization, termed a Pickering emulsion polymerization, is a practical way to prepare complex colloid structures.[104]

Armes and co-workers first reported the preparation of silica/polyaniline composites by using commercial ultrafine silica sols as the stabilizer in 1992.[105] The silica nanosols can also be used as a stabilizer for the in situ polymerization of various monomers to prepare raspberry-like hybrid microspheres.[106–114] Similar polymerizations of aniline with the different nanoparticles stabilizers, such as ZnO,[115] SiO_2,[116]and CeO_2,[117] can be used to prepare conducting polyaniline raspberry-like composites. Bon and co-workers used laponite clay as a stabilizer to fabricate clay-decorated PS latexes by a Pickering emulsion technique.[118] In their approach, the size of the complex colloidal particles could be controlled by varying the mass ratio of clay and styrene. Other hydrophobic monomers, for example styrene, lauryl (meth)-acrylate, butyl (meth)acrylate, octyl acrylate, and 2-ethyl hexyl acrylate, have been used as the inner phase.[119] TiO_2 nanoparticles and polymer microgels were also used as Pickering emulsifiers to prepare raspberry-like complex capsules.[120,121] Recently, Bon and co-workers further developed multilayered nanocomposite polymer colloids using the Pickering emulsion polymerization of methyl methacrylate.[122] By using a second conventional seeded emulsion polymerization step, more complex multilayered nanocomposite polymer colloids could be prepared (Figure 11).

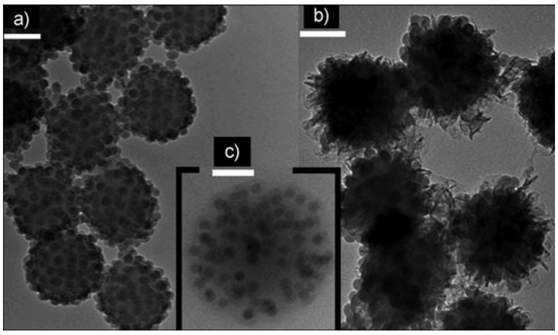

Figure 11. a) TEM images (scale bar: 100 nm) of poly (methyl methacrylate) latex armored with silica nanoparticles obtained by Pickering emulsion polymerization. b,c) Multilayered nanocomposite polymer colloids with b) a "hairy" outer layer of poly(acrylonitrile) and c) a soft shell of poly(*n*-butyl acrylate). Reprinted from Ref. [122] with permission. Copyright 2008 American Chemical Society.

Magnetic Fe_3O_4 nanoparticle-decorated PS microspheres were prepared by Wang et al.[123] Chen and co-workers used a similar strategy to prepare different particle-decorated polymer latexes.[124–127] Weitz and co-workers prepared responsive raspberry-like complex colloids with tunable permeability by covering the surface of temperature-sensitive microgels with colloidal particles.[128] Other than polymerization, Cayre and Biggs recently reported the preparation of hollow microspheres with a shell comprised of an inner polymeric porous membrane and an outer layer of nanoparticles; poly(methylmethacylate) was directly dissolved in the hexadecane/dichloromethane co-solvent as an oil phase.[129]

Water-in-oil emulsions stabilized with nanoparticles or colloid particles, termed inverse Pickering emulsions, have also been developed to generate complex colloid structures.[130–133] For example, Voorn and co-workers used a modified hydrophobic clay as the stabilizer to prepare poly(acrylamide)–clay nanocomposites.[130] Temperature-responsive SiO_2/poly(*N*-isopropylacrylamide) composite microspheres were prepared by inverse Pickering emulsion polymerization.[131,132] Colver and Bon reported the fabrication of cellular polymer monoliths by microgel-stabilized Pickering high-internal-emulsion polymerization.[134]

5.2. Aqueous-Phase Gelation

Aqueous-phase gelation combined with the Pickering emulsion method was used by several research groups to produce novel composite colloidosomes with gel cores and shells that consist of coagulated or partially fused colloid particles.[29,135–138] This method involves hydrophobic-nanoparticle- or colloidal-particle-stabilized water-in-oil Pickering emulsions and subsequent gelation of the aqueous core.

Paunov and co-workers reported the fabrication of agarose colloidosome gels with a shell of polymeric microrods in which a two-step procedure was used: Hot aqueous agarose solution was emulsified in tricaprylin in the presence of rodlike polymeric particles to produce a stable water-in-oil emulsion; the system was then cooled to obtain agarose gel covered with polymer microrod particles.[138] By this approach, a hairy raspberry structure was obtained (Figure 12a). If PS colloidal particles were added into the oil phase, agarose–gel colloidosomes could be produced with the PS colloids decorating the surface (Figure 12b).[139] Nanoparticles of materials such as Fe_3O_4 can also stabilize hot agarose solutions and, when the system is cooled to room temperature, nanoparticle-covered agarose–gel colloidosomes are produced.[29] Wang and co-workers found that when 4 nm CdS nanoparticles were encapsulated in the agarose gels stabilized with 8 nm Fe_3O_4 nanoparticles, the CdS nanoparticles could be released from the core into the aqueous solution.[29] When 4 nm and 2.8 nm CdS nanoparticles were both entrapped in the agarose gel core with 5 nm Fe_3O_4 nanoparticle stabilizers, only 2.8 nm CdS nanoparticles could be selectively released from the gels. This result suggests that the pore size of the colloidosome membranes can be varied by altering the size of the particles as well as by controlling the extent to which they fuse. Thus, the colloidosome core–shell gel-composite structures have great potential in controlling the release of entrapped molecules.

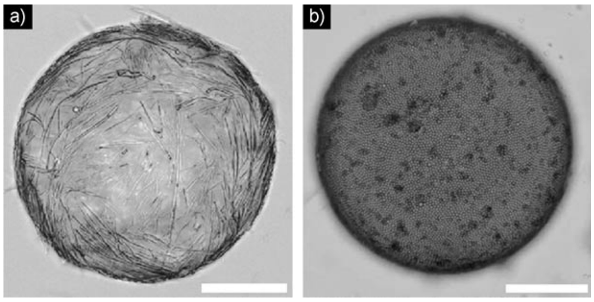

Figure 12. a) Optical microscope images of a microrod/agarose gel raspberry complex. Modified image; reprinted from Ref. [138] with permission. Copyright 2004 American Chemical Society. b) PS microspheres/agarose gel raspberry complex. Modified image; reprinted from Ref. [139] with permission. Copyright 2004 Royal Society of Chemistry. Scale bars: 100 μm.

Recently, Tong and co-workers further improved this method by using porous $CaCO_3$ microparticles as the stabilizer.[135] They added D-glucono-δ-lactone into the aqueous phase to lower the pH. As a result, Ca^{2+} ions were released to cross-link the alginate chains in the water phase, forming gel cores. This procedure can be performed at low temperature, which can decrease the effect of heating on the bioactivity of encapsulated materials. Subsequently, they encapsulated insulin in agarose gels that were stabilized with γ-Fe_2O_3 nanoparticles and studied the in vitro release behavior.[140]

6. Capsules, Thin Films, and Raspberry Composites by Self-Assembly of Bionanoparticles at Interfaces

Bionanoparticles (BNPs), such as viruses, ferritin, and other supramolecular protein assemblies, self-assemble by non-covalent interactions to become highly organized supramolecular systems.[141,142] BNPs offer a wide array of shapes, for example rods and spheres, with sizes ranging from tens to hundreds of nanometers. As monodispersed nanoparticles, BNPs are ideal model system to investigate self-assembly phenomenon.[143] Furthermore, the surface properties of BNPs can be easily manipulated chemically or genetically without disrupting the integrity of the particles. The presence of different surface functionalities and charges may greatly alter the assembly behavior of these particles. However, the basic principles underpinning the interfacial assembly should remain the same.

6.1. Capsules

Similar to the work with inorganic colloidal particles, Russell, Wang and co-workers, using cowpea mosaic virus (CPMV) and turnip yellow mosaic virus (TYMV), generated close-packed monolayers of virus particles at the oil–water interface (Figure 13).[10,144] CPMV and TYMV are both circa 30 nm-diameter plant viruses that can be inexpensively

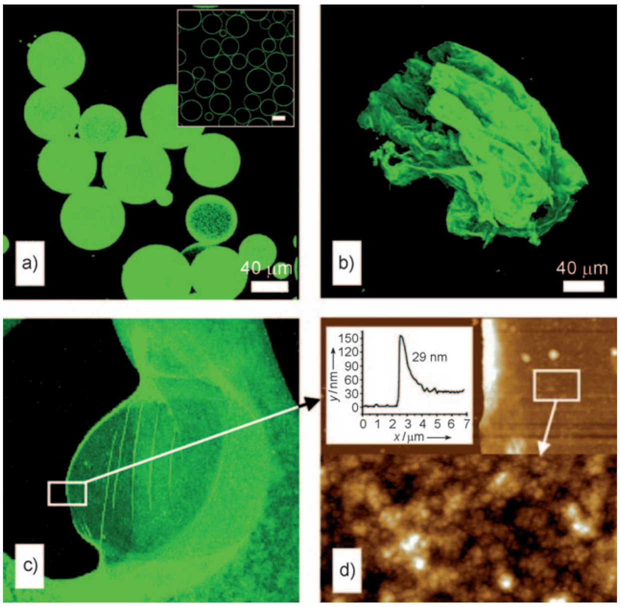

Figure 13. Confocal fluorescence microscope image of CPMV particle assembly after cross-linking with glutaraldehyde. a) 3D reconstruction of perfluorodecalin droplets in water; the droplets are coated with the virus (inset: cross-sectional view). Excess particles were removed by successive washing with water. b) Crumpled droplet after complete drying and rehydration with water. c) Capsule cap after complete drying. d) The white box shows the area at which the SFM scan was taken, and the lower part shows the height profile on top of the collapsed capsule (image width: 2 μm, *z* range: 30 nm). Reprinted from Ref. [144].

isolated in gram quantities from the infected plant leaves by simple purification methods. Unlike inorganic nanoparticles, which require functionalized ligands for cross-linking, CPMV, TYMV, and other BNPs have native functional groups that are chemically accessible, such as amines, carboxylic acids, and phenol groups. The in situ cross-linking between the assembled virus particles result in a stable virus-based membrane in which the integrity of viral particles is preserved (Figure 13 b). The cross-linking, as with the synthetic nanoparticles, stabilizes the assemblies by the covalent bonding.

Ferritin, a circa 12 nm diameter tetracosameric protein particle, can also be used as a Pickering emulsifier, forming a close-packed array on the droplet surface.[145] The interior cavity measures 7–8 nm in diameter and encapsulates a mineralized iron core. If the iron core is removed, this protein cage is called apoferritin. Ferritin can co-assemble with synthetic nanocrystals, such as CdSe, at the oil–water interface.[146] A sequential ring-opening metathesis polymerization process can cross-link the ferritins and form stable capsules and thin films. Similarly, Bausch and co-workers recently reported on the preparation of silk microcapsules by the interfacial adsorption of silk proteins.[147,148]

The tobacco mosaic virus (TMV), a rod-like bionanoparticle, can assume different orientations when assembled at the oil–water interface.[46] TMV is a rod-shaped plant virus composed of 2130 identical protein subunits arranged helically around a genomic single-strand RNA.[149] The diameter of a native TMV is 18 nm, with a length of about 300 nm that is defined by the length of the encapsulated genomic RNA. Depending on the initial TMV concentration, the orientation of these bionanorods assumes different orientations. At low concentrations, TMV orients parallel to the interface, whereas at higher concentrations, the TMV is oriented normal to the interface.[46] In combination with other assembly methods, interfacial assembly of TMV in a capillary tube can lead to more complex hierarchical structures.[150] Furthermore, the viral particles can be modified with various ligands and organized on various substrates to mimic the ligand distribution and complexity of the native tissue environment.[151]

6.2. Two-Dimensional Crystal-Like Arrays

Although the basic driving force to assemble nanoparticles at the interface of two immiscible liquids is to decrease interfacial energy, these nanoparticle assemblies are dynamic and thus lack in-plane order. Therefore, to generate long-range ordered 2D assemblies, a greatly retarded or arrested particle exchange is required. Fujiyoshi and co-workers demonstrated that ferritin at a planar interface of a positively charged amine, dehydroabietylamine (DHAA), in the organic phase (hexane) led to highly ordered hexagonally packed arrays of ferritin (apoferritin) and proteins.[152–154] These assemblies can be transferred to a solid support without losing the lateral order.[155] Recently, 2D crystallization of In-ferritin (ferritin with indium cores) was also reported (Figure 14 a).[156] Dps (DNA-binding proteins from starved cells, a 9 nm diameter dodecameric protein assembly) belong to the ferritin superfamily and are known to form a paracrystalline structure with DNA. Similar to ferritin, Dps particles can also self-assemble at the air–water interface and form a well-defined 2D crystal. (Figure 14 b).[157]

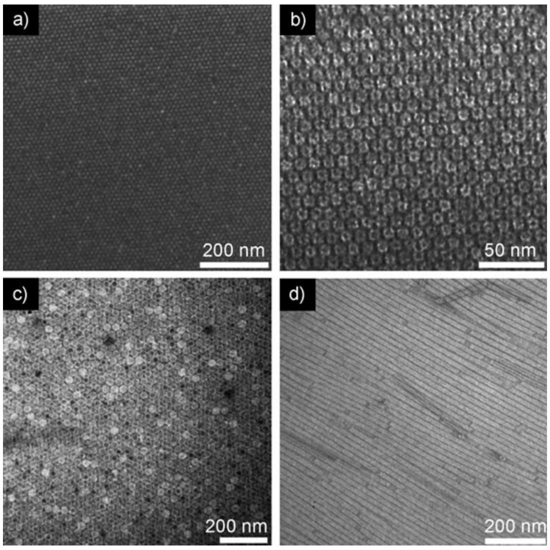

Figure 14. 2D crystals of BNPs. a) SEM image of ferritin with an indium core array on a silicon wafer. The array was formed at the air–water interface and was successfully transferred onto the silicon wafer. Reprinted from Ref. [156] with permission. Copyright 2005 American Chemical Society. b) TEM images of Dps arrays. The sample was stained with uranyl acetate. Reprinted from Ref. [157] with permission. Copyright 2006 Elsevier. c) TEM image of a 2D TYMV crystal. The arrays were formed at the water–heptane interfaces and were transferred onto a carbon-coated copper grid by a vertical transfer method. The sample was stained with uranyl acetate. Reprinted from Ref. [10] with permission. Copyright 2009 American Chemical Society. d) TEM images of 2D TMV arrays. A long-range parallel TMV 2D crystal was formed at the air–water interface and was successfully transferred onto a carbon-coated copper grid by a vertical transfer method. The sample was stained with uranyl acetate.

TYMV was also used to investigate assembly at flat oil–water interfaces.[10] At a planar interface, the adsorption–desorption kinetics can be manipulated by changing the viscosity of the system. By increasing the viscosity of the liquid(s), highly ordered arrays with long-range lateral order can be produced (Figure 14 c), cross-linked, and transferred to a solid support, underscoring the mechanical integrity of the cross-linked films. Similar strategies can be used to generate 2D arrays of rod-like TMVs (Figure 14 d).

6.3. Raspberry-Like Core–Shell Structures

In a similar concept to Pickering emulsion formation, certain polymers, such as poly(4-vinylpyridine) (P4VP), can be used as the organic phase to form composite structures. Wang and co-workers reported the co-assembly of BNPs with P4VP to form core–shell composite structures.[158–160] The hydrophobic polymer was initially dissolved in a polar organic solvent and mixed with an aqueous solution of virus particles. The evaporation of the organic solvent resulted in the formation of a spherical, hydrophobic polymer core decorated with the hydrophilic virus particles partially embedded in the polymer. The size distribution of the resultant virus-particle-decorated polymer spheres was controlled by the mass ratio of viral particles to polymer. When CPMV was used as the nanoparticle, a raspberry-like structure was produced (Figure 15 a).[158] Interestingly, when another spherical virus, TYMV, was used for the co-assembling with P4VP, the P4VP sphere was completely covered with a hexagonally close-packed array of the TYMV.[159] Although CPMV and TYMV are equal in size, the difference in surface charges and surface structures may cause the different interaction with P4VP. Other spherical-like BNPs, such as ferritin and bacteriophage P22, as well as rod-like virus TMV and bacteriophage M13, can also form core–shell composite structures upon assembling with P4VP (Figure 15 b).[160,161] This strategy offers a simple route to produce core–shell composite structures, which have potential applications in drug delivery and tissue engineering.

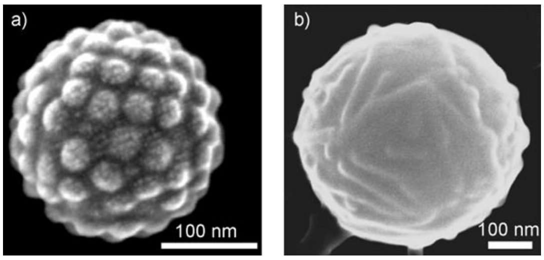

Figure 15. SEM images of core–shell structures generated by co-assembly of P4VP with a) CPMV and b) TMV. Both samples were coated with a thin layer of platinum and characterized with a high-resolution field-emission scanning electron microscopy.

7. Janus Structures and Interfacial Reactions

Janus particles, as the name implies, are heterogeneous in nature, being comprised of two dissimilar materials or having two different types of surface interactions, such as being hydrophobic in one part and hydrophilic in the other, or having two different types of charge.[32,162] As would be expected, Janus particles are similar in nature to a surfactant in which one part of the particle prefers one fluid and the other part another fluid when the fluids are immiscible. Janus particles can be produced by a variety of means, including the use of spherically confined phase-separated polymers, di- and triblock copolymers, selective modification by lithographic techniques, or continuous-flow lithography methods. Recently, the Pickering-emulsion-assisted synthesis of Janus colloids has aroused great attention owing to its diversity, simplicity, and most importantly, massive production.

Colloidal particles or nanoparticles can act as Pickering emulsifiers and absorb at the aqueous–organic interface. With one part of particle in the organic phase and the other in the aqueous phase, selective modification of the colloidal particles at interface can be achieved from either the organic or aqueous phase or both to produce Janus particles. For example, different inorganic Janus particles of Fe_3O_4 and Ag, Fe_3O_4 and Au, FePt and Ag, and Au and Ag were prepared by modification of nanoparticles at the oil–water interface by Xu and co-workers (Figure 16).[163] For the preparation of Fe_3O_4 and Ag Janus particles, Fe_3O_4 nanoparticles were first dissolved in a suitable organic solvent; the solution was then introduced into an aqueous solution of silver nitrate. After ultrasonification, a stable Pickering emulsion was formed in which the Fe_3O_4 nanoparticles were absorbed at the oil–water interface. Iron(II) in the aqueous solution acts as reductant for silver(I) and assists in the seeding of the silver nanoparticles.

A similar strategy was used to prepare Janus poly(*N*-isopropylacrylamide-*co*-acrylic acid) colloids with NH_2 in one part and COOH in another by use of an aqueous EDC coupling reaction (EDC = 1-ethyl-3-(3-dimethylaminopropyl)carbodiimide).[164] Janus silica particles decorated with biotin molecules and poly(ethylene oxide) chains on two hemispheres were prepared by two-step click reactions.[165] Recently, Yang and co-workers reported another approach to prepare Janus colloids by a simultaneous biphasic grafting of different polymer brushes onto the two parts of a Pickering colloid at a liquid–liquid emulsion interface by atom-transfer radical polymerization.[166]

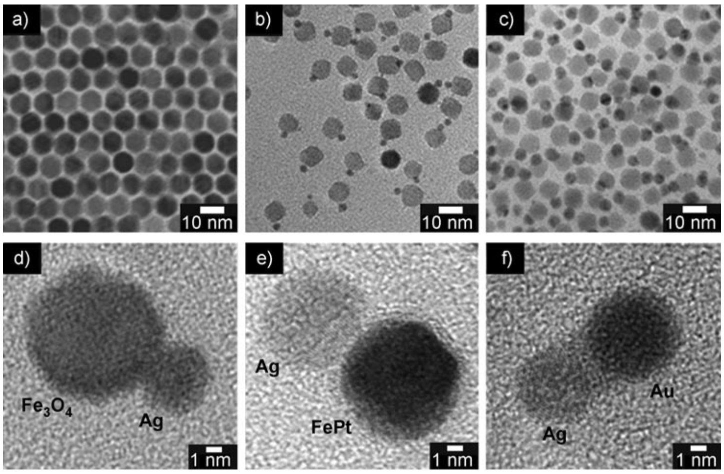

Figure 16. TEM images of a) the as-prepared Fe_3O_4 nanoparticles and b,c) the Fe_3O_4-Ag heterodimers after b) 10 min reaction and c) after the reaction stopped at 30 min. d–f) HRTEM images of Fe_3O_4-Ag (d), FePt-Ag (e), and Au-Ag (f). Reprinted from Ref. [163] with permission. Copyright 2005 American Chemical Society.

It is still unclear whether the rotation of the particles at the interface influences the formation of the Janus structure. To avoid particle rotation, a wax solidification method was developed by Granick and co-workers,[38] which involves imbedding the colloidal particles in a solid wax in contact with water. The aqueous unprotected part of the colloidal particles could be then selectively modified. By this method, silica particles were selectively modified with a silane to form Janus colloids.[38] This method can be extended to generate non-spherical Janus colloids. Recently, Yang et al. reported a simple approach to prepare non-spherical Janus colloids by an

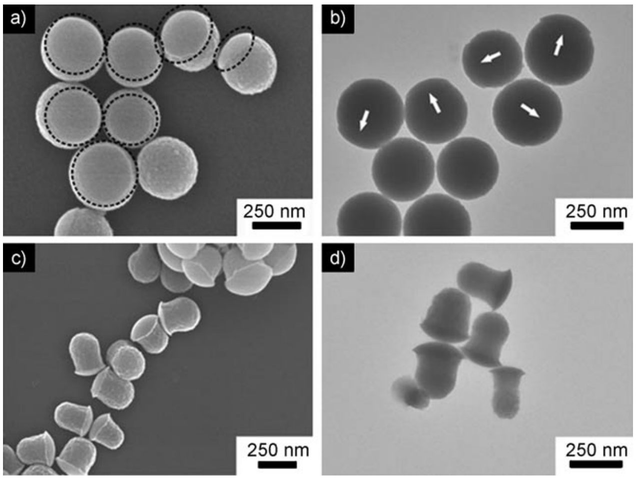

Figure 17. a, b) SEM and TEM images of spherical Janus silica colloids formed by asymmetric etching the silica-NH_2 colloid for 21 h. c, d) SEM and TEM images of the as-prepared mushroom-like Janus silica colloids by repeatedly etching for 42 days. Reprinted from Ref. [167] with permission. Copyright 2009 Royal Society of Chemistry.

asymmetric wet-etching (Figure 17).[167] The silica colloid was first modified with a silane to introduce a thin functional corona onto the silica surface. At the solidified wax–water interface, the colloids were partially embedded and protected. After the exposed part was selectively etched, a fresh silica surface with a Si–OH group was exposed. Janus spherical colloids were derived with Si–NH_2 in one part and Si–OH in another. By further increasing the etching time to 42 days, the spherical Janus colloids evolved into non-spherical mushroom-like structure. The Janus silica particles can also be used as a template to prepare Janus SiO_2/PS complex colloids. Janus CuO/CuS colloids were also successfully prepared using a precipitation reaction in the water phase of a Pickering emulsion.[168]

Apart from forming well-defined structure at interfaces, particle-containing interfaces can also be utilized as templates for the preparation of novel materials and as a reaction location for specific targeting. Gao and co-workers reported a interfacial layer-by-layer approach to prepare freestanding asymmetric metallic nanoparticles in thin films.[169] Specific DNA base pairing was employed to build up trilayer nanoparticle films of CdTe-Au-Ag by anchoring the central gold particles to the interface. Briefly, gold nanoparticles capped with ligands amenable to hydrogen bonding base pairing were first self-assembled at the oil–water interface. When complementary base-paring molecules were added, either from aqueous phase or oil phase, surface terminal groups of the gold nanoparticles were converted into SH or phosphate groups. The SH or phosphate groups can then react with CdTe or silver nanoparticles in the oil phase or aqueous phase, thus leading to asymmetric multilayered thin films of nanoparticles. This approach opens up a novel method to prepare asymmetric multilayer nanoparticle thin films with defined structures.

The self-assembled monolayers at oil–water interfaces can also foster organic reactions.[170] For example, orthogonally functionalized FePt nanoparticles were first self-assembled at the oil–water interface and cross-linked by dithiocarbamate chemistry, and a stable oil-in-water emulsion was obtained. Interfacial reactions were demonstrated by host–guest chemistry by encapsulation of a flavin polymer inside the microcapsules to obtain three-point hydrogen-bonding interaction at the interface with a complementary diaminopyridine amphiphile. Host–guest interactions at the interface were shown by monitoring fluorescence quenching of the flavin fluorophore upon addition of an excess of the guest diaminopyridine amphiphile.[170]

8. Conclusions

The air–liquid and liquid–liquid interfaces provide well-defined platforms to promote the assembly of nano- or microparticles, and the fluid nature of these interfaces allows the adsorbed particles to attain an equilibrium configuration. A further advantage of liquid interfaces is the ability to control the assembly by modifying the interparticle interactions by surface-property control of the particles. In this Review, many examples of assemblies at flat and curved interfaces have been described, including the generation of nanocrystalline films, colloidosomes, nanoparticle-decorated polymer latexes, and raspberry biocomposite structures. Interfacial assemblies and reactions can also be used to generate Janus particles, or even more complex structures.

The ability to control the assembly of colloidal and nanoparticles to achieve well-defined hierarchical structures is important for their ultimate applications. Scaling up interfacial assemblies can easily be envisioned by use of continuous flow of two fluids in a channel where the desired hierarchically assembled structures can be collected downstream. Establishing fundamental theoretical arguments and alternate routes toward interfacial assembly will further promote research to address more challenging issues. For example, one outstanding question is how the assembly and orientation of the anisotropic particles can be controlled at interface. Although some results were reported using rod-like anisotropic particles,[44,46] work in this area has only just begun. For example, ways to assemble bioactive proteins, protein assemblies, or DNA–protein complexes at liquid interfaces to afford predictable 3D superstructures while maintaining the bioactivities of the building blocks have not yet been explored. Clearly, the assemblies at air–liquid or liquid–liquid interfaces offer many opportunities to synthesize new materials with complex structural features and functions, which will rely on the collaborative endeavors of chemists, physicists, materials scientists, and engineers.

The work reported in references [10, 46, 158–161] was partially supported by the US NSF (DMR-0706431, CHE-0748690), the US Department of Energy Office of Basic Energy, the Alfred P. Sloan Scholarship, the Camille Dreyfus Teacher Scholar Award, US-ARO (W911NF-04-1-019 and W911NF-09-1-236), and the W. M. Keck Foundation.

Received: March 18, 2010

[1] J. E. Green, J. W. Choi, A. Boukai, Y. Bunimovich, E. Johnston-Halperin, E. DeIonno, Y. Luo, B. A. Sheriff, K. Xu, Y. S. Shin, H. R. Tseng, J. F. Stoddart, J. R. Heath, *Nature* **2007**, *445*, 414.

[2] R. J. Jackman, J. L. Wilbur, G. M. Whitesides, *Science* **1995**, *269*, 664.

[3] S. Kinge, M. Crego-Calama, D. N. Reinhoudt, *ChemPhysChem* **2008**, *9*, 20.

[4] A. Böker, J. He, T. Emrick, T. P. Russell, *Soft Matter* **2007**, *3*, 1231.

[5] F. Bresme, M. Oettel, *J. Phys. Condens. Matter* **2007**, *19*, 413101.

[6] S. U. Pickering, *J. Chem. Soc.* **1907**, *91*, 940.

[7] W. Ramsden, *Proc. R. Soc. London* **1903**, *72*, 156.

[8] C. N. R. Rao, K. P. Kalyanikutty, *Acc. Chem. Res.* **2008**, *41*, 489.

[9] S. Acharya, J. P. Hill, K. Ariga, *Adv. Mater.* **2009**, *21*, 2959.

[10] G. Kaur, J. B. He, J. Xu, S. V. Pingali, G. Jutz, A. Böker, Z. W. Niu, T. Li, D. Rawlinson, T. Emrick, B. Lee, P. Thiyagarajan, T. P. Russell, Q. Wang, *Langmuir* **2009**, *25*, 5168.

[11] K. J. M. Bishop, C. E. Wilmer, S. Soh, B. A. Grzybowski, *Small* **2009**, *5*, 1600.

[12] C. Zeng, H. Bissig, A. D. Dinsmore, *Solid State Commun.* **2006**, *139*, 547.

[13] W. H. Binder, *Angew. Chem.* **2005**, *117*, 5300; *Angew. Chem. Int. Ed.* **2005**, *44*, 5172.

[14] D. L. Cheung, S. A. F. Bon, *Phys. Rev. Lett.* **2009**, *102*, 066103.

[15] F. Reincke, W. K. Kegel, H. Zhang, M. Nolte, D. Y. Wang, D. Vanmaekelbergh, H. Möhwald, *Phys. Chem. Chem. Phys.* **2006**, *8*, 3828.

[16] H. Zhang, E. W. Edwards, D. Y. Wang, H. Möhwald, *Phys. Chem. Chem. Phys.* **2006**, *8*, 3288.

[17] E. Glogowski, R. Tangirala, T. P. Russell, T. Emrick, *J. Polym. Sci. Part A* **2006**, *44*, 5076.

[18] N. Popp, S. Kutuzov, A. Böker, *Adv. Polym. Sci.* **2010**, *228*, 39.

[19] P. Pieranski, *Phys. Rev. Lett.* **1980**, *45*, 569.

[20] Y. Lin, A. Böker, H. Skaff, D. Cookson, A. D. Dinsmore, T. Emrick, T. P. Russell, *Langmuir* **2005**, *21*, 191.

[21] B. P. Binks, S. O. Lumsdon, *Langmuir* **2000**, *16*, 8622.

[22] B. P. Binks, S. O. Lumsdon, *Langmuir* **2001**, *17*, 4540.

[23] B. P. Binks, C. P. Whitby, *Langmuir* **2004**, *20*, 1130.

[24] T. S. Horozov, R. Aveyard, J. H. Clint, B. P. Binks, *Langmuir* **2003**, *19*, 2822.

[25] J. Giermanska-Kahn, V. Schmitt, B. P. Binks, F. Leal-Calderon, *Langmuir* **2002**, *18*, 2515.

[26] H. W. Duan, D. A. Wang, D. G. Kurth, H. Möhwald, *Angew. Chem.* **2004**, *116*, 5757; *Angew. Chem. Int. Ed.* **2004**, *43*, 5639.

[27] Y. Lin, H. Skaff, T. Emrick, A. D. Dinsmore, T. P. Russell, *Science* **2003**, *299*, 226.

[28] D. Y. Wang, H. Möhwald, *J. Mater. Chem.* **2004**, *14*, 459.

[29] H. W. Duan, D. Y. Wang, N. S. Sobal, M. Giersig, D. G. Kurth, H. Möhwald, *Nano Lett.* **2005**, *5*, 949.

[30] J. H. Schulmann, J. Leja, *Trans. Faraday Soc.* **1954**, *50*, 598.

[31] R. Aveyard, J. H. Clint, T. S. Horozov, *Phys. Chem. Chem. Phys.* **2003**, *5*, 2398.

[32] B. P. Binks, P. D. I. Fletcher, *Langmuir* **2001**, *17*, 4708.

[33] E. Duguet, C. Poncet-Legrand, S. Raviane, E. Bourgeat-Lami, S. Reculusa, C. Mingotaud, M. H. Delville, F. Pereira, WO 2005/049195, France, **2005**.

[34] R. Erhardt, A. Böker, H. Zettl, H. Kaya, W. Pyckhout-Hintzen, G. Krausch, V. Abetz, A. H. E. Müller, *Macromolecules* **2001**, *34*, 1069.

[35] R. Erhardt, M. F. Zhang, A. Böker, H. Zettl, C. Abetz, P. Frederik, G. Krausch, V. Abetz, A. H. E. Müller, *J. Am. Chem. Soc.* **2003**, *125*, 3260.

[36] S. Förster, M. Antonietti, *Adv. Mater.* **1998**, *10*, 195.

[37] H. W. Gu, R. K. Zheng, X. X. Zhang, B. Xu, *J. Am. Chem. Soc.* **2004**, *126*, 5664.

[38] L. Hong, S. Jiang, S. Granick, *Langmuir* **2006**, *22*, 9495.

[39] Y. Li, Q. Zhang, A. V. Nurmikko, S. H. Sun, *Nano Lett.* **2005**, *5*, 1689.

[40] Z. F. Li, D. Y. Lee, M. F. Rubner, R. E. Cohen, *Macromolecules* **2005**, *38*, 7876.

[41] A. Perro, S. Reculusa, S. Ravaine, E. B. Bourgeat-Lami, E. Duguet, *J. Mater. Chem.* **2005**, *15*, 3745.

[42] S. Schrage, R. Sigel, H. Schlaad, *Macromolecules* **2003**, *36*, 1417.

[43] T. Teranishi, Y. Inoue, M. Nakaya, Y. Oumi, T. Sano, *J. Am. Chem. Soc.* **2004**, *126*, 9914.

[44] J. He, Q. Zhang, S. Gupta, T. Emrick, T. R. Russell, P. Thiyagarajan, *Small* **2007**, *3*, 1214.

[45] S. Kutuzov, J. He, R. Tangirala, T. Emrick, T. P. Russell, A. Böker, *Phys. Chem. Chem. Phys.* **2007**, *9*, 6351.

[46] J. B. He, Z. W. Niu, R. Tangirala, J. Y. Wan, X. Y. Wei, G. Kaur, Q. Wang, G. Jutz, A. Böker, B. Lee, S. V. Pingali, P. Thiyagarajan, T. Emrick, T. P. Russell, *Langmuir* **2009**, *25*, 4979.

[47] L. C. Dong, D. T. Johnson, *Langmuir* **2005**, *21*, 3838.

[48] M. E. Leunissen, A. van Blaaderen, A. D. Hollingsworth, M. T. Sullivan, P. M. Chaikin, *Proc. Natl. Acad. Sci. USA* **2007**, *104*, 2585.

[49] A. R. Tao, J. X. Huang, P. D. Yang, *Acc. Chem. Res.* **2008**, *41*, 1662.

[50] K. M. Gattas-Asfura, C. A. Constantine, M. J. Lynn, D. A. Thimann, X. J. Ji, R. M. Leblanc, *J. Am. Chem. Soc.* **2005**, *127*, 14640.

[51] H. J. Chen, S. J. Dong, *Langmuir* **2007**, *23*, 12503.

[52] Y. Y. Yang, S. Pradhan, S. W. Chen, *J. Am. Chem. Soc.* **2004**, *126*, 76.

[53] P. R. Selvakannan, A. Swami, D. Srisathiyanarayanan, P. S. Shirude, R. Pasricha, A. B. Mandale, M. Sastry, *Langmuir* **2004**, *20*, 7825.

[54] D. K. Lee, Y. H. Kim, C. W. Kim, H. G. Cha, Y. S. Kang, *J. Phys. Chem. B* **2007**, *111*, 9288.

[55] F. Kim, S. Kwan, J. Akana, P. D. Yang, *J. Am. Chem. Soc.* **2001**, *123*, 4360.

[56] S. Acharya, S. Efrima, *J. Am. Chem. Soc.* **2005**, *127*, 3486.

[57] A. Tao, F. Kim, C. Hess, J. Goldberger, R. R. He, Y. G. Sun, Y. N. Xia, P. D. Yang, *Nano Lett.* **2003**, *3*, 1229.

[58] X. L. Li, L. Zhang, X. R. Wang, I. Shimoyama, X. M. Sun, W. S. Seo, H. J. Dai, *J. Am. Chem. Soc.* **2007**, *129*, 4890.

[59] H. J. Tsai, Y. L. Lee, *Soft Matter* **2009**, *5*, 2962.

[60] N. A. Melosh, A. Boukai, F. Diana, B. Gerardot, A. Badolato, P. M. Petroff, J. R. Heath, *Science* **2003**, *300*, 112.

[61] Z. H. Zhong, D. L. Wang, Y. Cui, M. W. Bockrath, C. M. Lieber, *Science* **2003**, *302*, 1377.

[62] F. Patolsky, B. P. Timko, G. H. Yu, Y. Fang, A. B. Greytak, G. F. Zheng, C. M. Lieber, *Science* **2006**, *313*, 1100.

[63] S. Jin, D. M. Whang, M. C. McAlpine, R. S. Friedman, Y. Wu, C. M. Lieber, *Nano Lett.* **2004**, *4*, 915.

[64] J. L. Hernandez-Lopez, E. R. Alvizo-Paez, S. E. Moya, J. Ruiz-Garcia, *J. Phys. Chem. B* **2006**, *110*, 23179.

[65] H. Xia, D. Wang, *Adv. Mater.* **2008**, *20*, 4253.

[66] T. P. Bigioni, X. M. Lin, T. T. Nguyen, E. I. Corwin, T. A. Witten, H. M. Jaeger, *Nat. Mater.* **2006**, *5*, 265.

[67] K. E. Mueggenburg, X. M. Lin, R. H. Goldsmith, H. M. Jaeger, *Nat. Mater.* **2007**, *6*, 656.

[68] F. Reincke, S. G. Hickey, W. K. Kegel, D. Vanmaekelbergh, *Angew. Chem.* **2004**, *116*, 464; *Angew. Chem. Int. Ed.* **2004**, *43*, 458.

[69] P. Arumugam, D. Patra, B. Samanta, S. S. Agasti, C. Subramani, V. M. Rotello, *J. Am. Chem. Soc.* **2008**, *130*, 10046.

[70] L. J. Xu, G. B. Han, J. W. Hu, Y. He, J. G. Pan, Y. J. Li, J. N. Xiang, *Phys. Chem. Chem. Phys.* **2009**, *11*, 6490.

[71] J. Wang, D. Y. Wang, N. S. Sobal, M. Giersig, M. Jiang, H. Mohwald, *Angew. Chem.* **2006**, *118*, 8131; *Angew. Chem. Int. Ed.* **2006**, *45*, 7963.

[72] S. Biswas, L. T. Drzal, *Nano Lett.* **2009**, *9*, 167.

[73] Y. J. Zhang, Y. F. Shen, D. Kuehner, S. X. Wu, Z. M. Su, S. Ye, L. Niu, *Chem. Commun.* **2008**, 4273.
[74] P. Asuri, S. S. Karajanagi, J. S. Dordick, R. S. Kane, *J. Am. Chem. Soc.* **2006**, *128*, 1046.
[75] J. Matsui, K. Yamamoto, T. Miyashita, *Carbon* **2009**, *47*, 1444.
[76] J. Matsui, K. Yamamoto, N. Inokuma, H. Orikasa, T. Kyotani, T. Miyashita, *Mol. Cryst. Liq. Cryst.* **2008**, *491*, 9.
[77] J. Matsui, K. Yamamoto, N. Inokuma, H. Orikasa, T. Kyotani, T. Miyashita, *J. Mater. Chem.* **2007**, *17*, 3806.
[78] L. F. Hu, R. Z. Ma, T. C. Ozawa, F. X. Geng, N. Iyi, T. Sasaki, *Chem. Commun.* **2008**, 4897.
[79] O. D. Velev, K. Furusawa, K. Nagayama, *Langmuir* **1996**, *12*, 2374.
[80] A. D. Dinsmore, M. F. Hsu, M. G. Nikolaides, M. Marquez, A. R. Bausch, D. A. Weitz, *Science* **2002**, *298*, 1006.
[81] V. D. Gordon, C. Xi, J. W. Hutchinson, A. R. Bausch, M. Marquez, D. A. Weitz, *J. Am. Chem. Soc.* **2004**, *126*, 14117.
[82] L. M. Croll, H. D. H. Stover, *Langmuir* **2003**, *19*, 5918.
[83] X. D. He, X. W. Ge, M. Z. Wang, Z. C. Zhang, *J. Colloid Interface Sci.* **2006**, *299*, 791.
[84] X. D. He, X. W. W. Ge, M. Z. Wang, Z. C. Zhang, *Polymer* **2005**, *46*, 7598.
[85] X. D. He, X. W. Ge, H. R. Liu, H. X. Zhou, Z. C. Zhang, *Colloids Surf. A* **2007**, *301*, 80.
[86] X. D. He, X. W. Ge, H. R. Liu, M. G. Deng, Z. C. Zhang, *J. Appl. Polym. Sci.* **2007**, *105*, 1018.
[87] B. P. Binks, R. Murakami, *Nat. Mater.* **2006**, *5*, 865.
[88] S. Fujii, E. S. Read, B. P. Binks, S. P. Armes, *Adv. Mater.* **2005**, *17*, 1014.
[89] B. P. Binks, R. Murakami, S. P. Armes, S. Fujii, *Angew. Chem.* **2005**, *117*, 4873; *Angew. Chem. Int. Ed.* **2005**, *44*, 4795.
[90] B. P. Binks, T. S. Horozov, *Angew. Chem.* **2005**, *117*, 3788; *Angew. Chem. Int. Ed.* **2005**, *44*, 3722.
[91] Y. Lin, H. Skaff, A. Böker, A. D. Dinsmore, T. Emrick, T. P. Russell, *J. Am. Chem. Soc.* **2003**, *125*, 12690.
[92] H. Skaff, Y. Lin, R. Tangirala, K. Breitenkamp, A. Böker, T. P. Russell, T. Emrick, *Adv. Mater.* **2005**, *17*, 2082.
[93] E. Glogowski, R. Tangirala, J. B. He, T. P. Russell, T. Emrick, *Nano Lett.* **2007**, *7*, 389.
[94] D. Patra, F. Ozdemir, O. R. Miranda, B. Samanta, A. Sanyal, V. M. Rotello, *Langmuir* **2009**, *25*, 13852.
[95] B. Samanta, D. Patra, C. Subramani, Y. Ofir, G. Yesilbag, A. Sanyal, V. M. Rotello, *Small* **2009**, *5*, 685.
[96] N. Saleh, T. Sarbu, K. Sirk, G. V. Lowry, K. Matyjaszewski, R. D. Tilton, *Langmuir* **2005**, *21*, 9873.
[97] R. K. Wang, R. D. Reeves, K. J. Ziegler, *J. Am. Chem. Soc.* **2007**, *129*, 15124.
[98] R. K. Wang, H. O. Park, W. C. Chen, C. Silvera-Batista, R. D. Reeves, J. E. Butler, K. J. Ziegler, *J. Am. Chem. Soc.* **2008**, *130*, 14721.
[99] H. Ma, L. L. Dai, *Langmuir* **2009**, *25*, 11210.
[100] Z. H. Nie, J. Il Park, W. Li, S. A. F. Bon, E. Kumacheva, *J. Am. Chem. Soc.* **2008**, *130*, 16508.
[101] J. I. Park, Z. Nie, A. Kumachev, A. I. Abdelrahman, B. R. Binks, H. A. Stone, E. Kumacheva, *Angew. Chem.* **2009**, *121*, 5404; *Angew. Chem. Int. Ed.* **2009**, *48*, 5300.
[102] D. Lee, D. A. Weitz, *Adv. Mater.* **2008**, *20*, 3498.
[103] D. Lee, D. A. Weitz, *Small* **2009**, *5*, 1932.
[104] F. J. Rossier-Miranda, C. G. P. H. Schroen, R. M. Boom, *Colloids Surf. A* **2009**, *343*, 43.
[105] M. Gill, J. Mykytiuk, S. P. Armes, J. L. Edwards, T. Yeates, P. J. Moreland, C. Mollett, *J. Chem. Soc. Chem. Commun.* **1992**, 108.
[106] C. Barthet, A. J. Hickey, D. B. Cairns, S. P. Armes, *Adv. Mater.* **1999**, *11*, 408.
[107] S. Maeda, S. P. Armes, *J. Mater. Chem.* **1994**, *4*, 935.
[108] M. J. Percy, C. Barthet, J. C. Lobb, M. A. Khan, S. F. Lascelles, M. Vamvakaki, S. P. Armes, *Langmuir* **2000**, *16*, 6913.
[109] M. J. Percy, S. P. Armes, *Langmuir* **2002**, *18*, 4562.
[110] J. I. Amalvy, M. J. Percy, S. P. Armes, C. A. P. Leite, F. Galembeck, *Langmuir* **2005**, *21*, 1175.
[111] A. Schmid, J. Tonnar, S. P. Armes, *Adv. Mater.* **2008**, *20*, 3331.
[112] M. J. Percy, V. Michailidou, S. P. Armes, C. Perruchot, J. F. Watts, S. J. Greaves, *Langmuir* **2003**, *19*, 2072.
[113] M. J. Percy, J. I. Amalvy, D. P. Randall, S. P. Armes, S. J. Greaves, J. F. Watts, *Langmuir* **2004**, *20*, 2184.
[114] D. Dupin, A. Schmid, J. A. Balmer, S. P. Armes, *Langmuir* **2007**, *23*, 11812.
[115] J. Jeng, T. Y. Chen, C. F. Lee, N. Y. Liang, W. Y. Chiu, *Polymer* **2008**, *49*, 3265.
[116] Y. J. He, X. Y. Yu, *Mater. Lett.* **2007**, *61*, 2071.
[117] Y. J. He, *Mater. Chem. Phys.* **2005**, *92*, 134.
[118] S. Cauvin, P. J. Colver, S. A. F. Bon, *Macromolecules* **2005**, *38*, 7887.
[119] S. A. F. Bon, P. J. Colver, *Langmuir* **2007**, *23*, 8316.
[120] T. Chen, P. J. Colver, S. A. F. Bon, *Adv. Mater.* **2007**, *19*, 2286.
[121] S. A. F. Bon, S. Cauvin, P. J. Colver, *Soft Matter* **2007**, *3*, 194.
[122] P. J. Colver, C. A. L. Colard, S. A. F. Bon, *J. Am. Chem. Soc.* **2008**, *130*, 16850.
[123] C. Y. Wang, C. J. Zhang, Y. Li, Y. H. Chen, Z. Tong, *React. Funct. Polym.* **2009**, *69*, 750.
[124] Y. H. Zhang, H. Chen, X. W. Shu, Q. Zou, M. Chen, *Colloids Surf. A* **2009**, *350*, 26.
[125] Y. H. Zhang, Q. C. Zou, X. W. Shu, Q. Q. Tang, M. Chen, L. M. Wu, *J. Colloid Interface Sci.* **2009**, *336*, 544.
[126] M. Chen, L. M. Wu, S. X. Zhou, B. You, *Macromolecules* **2004**, *37*, 9613.
[127] M. Chen, S. X. Zhou, B. You, L. M. Wu, *Macromolecules* **2005**, *38*, 6411.
[128] J. W. Kim, A. Fernandez-Nieves, N. Dan, A. S. Utada, M. Marquez, D. A. Weitz, *Nano Lett.* **2007**, *7*, 2876.
[129] O. J. Cayre, S. Biggs, *J. Mater. Chem.* **2009**, *19*, 2724.
[130] D. J. Voorn, W. Ming, A. M. van Herk, *Macromolecules* **2006**, *39*, 2137.
[131] L. L. Duan, M. Chen, S. X. Zhou, L. M. Wu, *Langmuir* **2009**, *25*, 3467.
[132] Q. X. Gao, C. Y. Wang, H. X. Liu, C. H. Wang, X. X. Liu, Z. Tong, *Polymer* **2009**, *50*, 2587.
[133] F. F. Fang, H. J. Choi, Y. Seo, *J. Nanosci. Nanotechnol.* **2010**, *10*, 285.
[134] P. J. Colver, S. A. F. Bon, *Chem. Mater.* **2007**, *19*, 1537.
[135] C. Y. Wang, H. X. Liu, Q. X. Gao, X. X. Liu, Z. Tong, *Chemphyschem* **2007**, *8*, 1157.
[136] H. X. Liu, C. Y. Wang, Q. X. Gao, X. X. Liu, Z. Tong, *Int. J. Pharm.* **2008**, *351*, 104.
[137] C. Y. Wang, H. X. Liu, Q. X. Gao, X. X. Liu, Z. Tong, *Carbohydr. Polym.* **2008**, *71*, 476.
[138] P. F. Noble, O. J. Cayre, R. G. Alargova, O. D. Velev, V. N. Paunov, *J. Am. Chem. Soc.* **2004**, *126*, 8092.
[139] O. J. Cayre, P. F. Noble, V. N. Paunov, *J. Mater. Chem.* **2004**, *14*, 3351.
[140] H. X. Liu, C. Y. Wang, Q. X. Gao, J. X. Chen, B. Y. Ren, X. X. Liu, Z. Tong, *Int. J. Pharm.* **2009**, *376*, 92.
[141] T. Douglas, M. Young, *Science* **2006**, *312*, 873.
[142] L. A. Lee, Q. Wang, *Nanomedicine* **2006**, *2*, 137.
[143] M. Fischlechner, E. Donath, *Angew. Chem.* **2007**, *119*, 3246; *Angew. Chem. Int. Ed.* **2007**, *46*, 3184.
[144] J. T. Russell, Y. Lin, A. Böker, L. Su, P. Carl, H. Zettl, J. B. He, K. Sill, R. Tangirala, T. Emrick, K. Littrell, P. Thiyagarajan, D. Cookson, A. Fery, Q. Wang, T. P. Russell, *Angew. Chem.* **2005**, *117*, 2472; *Angew. Chem. Int. Ed.* **2005**, *44*, 2420.
[145] S. Fujii, A. Aichi, M. Muraoka, N. Kishimoto, K. Iwahori, Y. Nakamura, I. Yamashita, *J. Colloid Interface Sci.* **2009**, *338*, 222.
[146] R. Tangirala, Y. X. Hu, M. Joralemon, Q. L. Zhang, J. B. He, T. P. Russell, T. Emrick, *Soft Matter* **2009**, *5*, 1048.

[147] K. D. Hermanson, M. B. Harasim, T. Scheibel, A. R. Bausch, *Phys. Chem. Chem. Phys.* **2007**, *9*, 6442.

[148] K. D. Hermanson, D. Huemmerich, T. Scheibel, A. R. Bausch, *Adv. Mater.* **2007**, *19*, 1810.

[149] A. Klug, *Philos. Trans. R. Soc. London Ser. B* **1999**, *354*, 531.

[150] Y. Lin, E. Balizan, L. A. Lee, Z. W. Niu, Q. Wang, *Angew. Chem.* **2010**, *122*, 880; *Angew. Chem. Int. Ed.* **2010**, *49*, 868.

[151] M. A. Bruckman, G. Kaur, L. A. Lee, F. Xie, J. Sepulvecla, R. Breitenkamp, X. Zhang, M. Joralemon, T. P. Russell, T. Emrick, Q. Wang, *ChemBioChem* **2008**, *9*, 519.

[152] K. Aoyama, K. Ogawa, Y. Kimura, Y. Fujiyoshi, *Ultramicroscopy* **1995**, *57*, 345.

[153] T. Scheybani, H. Yoshimura, W. Baumeister, K. Nagayama, *Langmuir* **1996**, *12*, 431.

[154] H. Yoshimura, *Adv. Biophys.* **1997**, *34*, 93.

[155] I. Yamashita, *Thin Solid Films* **2001**, *393*, 12.

[156] M. Okuda, Y. Kobayashi, K. Suzuki, K. Sonoda, T. Kondoh, A. Wagawa, A. Kondo, H. Yoshimura, *Nano Lett.* **2005**, *5*, 991.

[157] H. Yoshimura, *Colloids Surf. A* **2006**, *282*, 464.

[158] T. Li, Z. W. Niu, T. Emrick, T. R. Russell, Q. Wang, *Small* **2008**, *4*, 1624.

[159] T. Li, B. Ye, Z. W. Niu, P. Thompson, S. Seifert, B. Lee, Q. Wang, *Chem. Mater.* **2009**, *21*, 1046.

[160] T. Li, L. Y. Wu, N. Suthiwangcharoen, M. A. Bruckman, D. Cash, J. S. Hudson, S. Ghoshroy, Q. Wang, *Chem. Commun.* **2009**, 2869.

[161] T. Li, Z. W. Niu, N. Suthiwangcharoen, R. Li, P. E. Prevelige, Q. Wang, *Sci. China Ser. B* **2010**, *53*, 71.

[162] D. L. Cheung, S. A. F. Bon, *Soft Matter* **2009**, *5*, 3969.

[163] H. W. Gu, Z. M. Yang, J. H. Gao, C. K. Chang, B. Xu, *J. Am. Chem. Soc.* **2005**, *127*, 34.

[164] D. Suzuki, S. Tsuji, H. Kawaguchi, *J. Am. Chem. Soc.* **2007**, *129*, 8088.

[165] J. Zhang, X. J. Wang, D. X. Wu, L. Liu, H. Y. Zhao, *Chem. Mater.* **2009**, *21*, 4012.

[166] B. Liu, W. Wei, X. Z. Qu, Z. H. Yang, *Angew. Chem.* **2008**, *120*, 4037; *Angew. Chem. Int. Ed.* **2008**, *47*, 3973.

[167] B. Liu, C. L. Zhang, J. G. Liu, X. Z. Qu, Z. Z. Yang, *Chem. Commun.* **2009**, 3871.

[168] D. Li, Y. J. He, S. Wang, *J. Phys. Chem. C* **2009**, *113*, 12927.

[169] B. Wang, M. Wang, H. Zhang, N. S. Sobal, W. Tong, C. Gao, Y. Wang, M. Giersig, D. Wang, H. Mohwald, *Phys. Chem. Chem. Phys.* **2007**, *9*, 6313.

[170] D. Patra, C. Pagliuca, C. Subramani, B. Samanta, S. S. Agasti, N. Zainalabdeen, S. T. Caldwell, G. Cooke, V. M. Rotello, *Chem. Commun.* **2009**, 4248.